Distributed generation: Thermodynamic model for a solar-dish micro-gas turbine system

A. Medina[a], J. García-Ferrero[b], R.P. Merchán[c], M.J. Santos[d] and A. Calvo-Hernández[e]

[a] *University of Salamanca, Salamanca, Spain , amd385@usal.es*
[b] *University of Salamanca, Salamanca, Spain, jgferrero@usal.es*
[c] *University of Salamanca, Salamanca, Spain, rpmerchan@usal.es*
[d] *University of Salamanca, Salamanca, Spain, smjesus@usal.es*
[e] *University of Salamanca, Salamanca, Spain, anca@usal.es*

Abstract:

In this work a thermodynamic model that describes the performance of a power plant based on a hybrid recuperative Brayton-type parabolic dish is presented. The model is capable to analyse the performance of such plants at off-design conditions. One of the characteristics of parabolic dishes operating in hybrid mode is that they can work uninterruptedly, since the energy necessary for their operation comes from two different sources: a renewable one, the solar system, and a conventional one, the combustion of a fossil fuel. The use of a renewable energy source allows for the reduction of the fuel consumption and consequently of the emissions of pollutant gases. The distributed generation of electrical energy (that is, the installation of electricity production sources near where it is going to be used) motivates the development and optimization of these systems. The transformation of thermal energy to mechanical one is carried out by means of a Brayton thermodynamic cycle. The irreversibilities taking place in all subsystems (solar part, combustion chamber, micro-gas turbine, and the corresponding heat exchangers) have been considered in the model with home-software elaborated using Mathematica®. The model is validated by comparing with several results from the literature. Subsequently, an analysis is made for two operating conditions: with and without solar contributions. Four days are analysed, each of them corresponding to a season and for four different micro-turbine power outlets (30, 23, 15 and 7 kWe). In addition, an off-design study of the behaviour of the system is made for a representative day. An estimation of the greenhouse effect emissions is made, comparing the operation with and without solar power input.

Keywords:
Solar Parabolic Dish, Distributed Generation, Micro-Gas Turbine, Thermodynamic Model.

1. Introduction

Because of the increasing demand of electric energy associated with the also increasing world population and the need for reducing emissions of pollutant gases that are discharged into the atmosphere, international agreements and treaties (such as the 2016 Paris Agreement [1]) promote the use of renewable energy sources as a fundamental step in the search for a sustainable development.

Within the so-called clean energies (hydroelectric, wind, tidal, biomass, etc.), the present study is focused on solar thermal energy. As it is known, the Sun is the most abundant source of renewable energy [2] and Spain is one of the most propitious countries for this type of facilities because of its climatological conditions and because of the available solar irradiance (Fig. 1 left). The solar thermal energy is based on the use of the Sun as a heat source to obtain, through a thermal power block, a work that is used by an alternator to provide electrical energy at the end of the process.

There are currently different solar thermal systems depending on how the solar energy concentration process is carried out: central tower solar power plant, parabolic troughs, Fresnel linear reflectors, parabolic dish, etc. With the aim of avoiding power output fluctuations due to seasonal, meteorological conditions or during the night, two options are being investigated: thermal

storage and hybridization. This work deals with the last one, which takes advantage of solar power for favourable irradiance conditions and is completed, when necessary, burning fossil fuel to heat the working fluid before entering in the expansion process.

One of the high-temperature solar thermal generation systems is the parabolic dish concentrator system, which together with a Stirling or a Brayton cycle, allows for the transformation of thermal and mechanical energy into electrical. Currently, this technology is at the development stage, and innovative designs are needed to ensure efficient and reliable operation [3,4].

This study presents a thermodynamic model for a hybrid system constituted by a micro gas-turbine located at the parabolic dish collector focal point. It includes an algorithm developed with the *Mathematica*® tool considering the losses due to irreversibilities in each of the subsystems and in the heat exchangers. On-design and dynamical off-design predictions can be done, for any place and any meteorological condition. This will allow to determine the performance of the components of the system and then to focus the interest on several aspects to be improved and optimized.

1.1. Parabolic dish micro gas Turbine

The parabolic (dish) collector is composed of several elements (Fig. 1 right) such as the receiver, absorber, solar tracking system, support structure, and other:

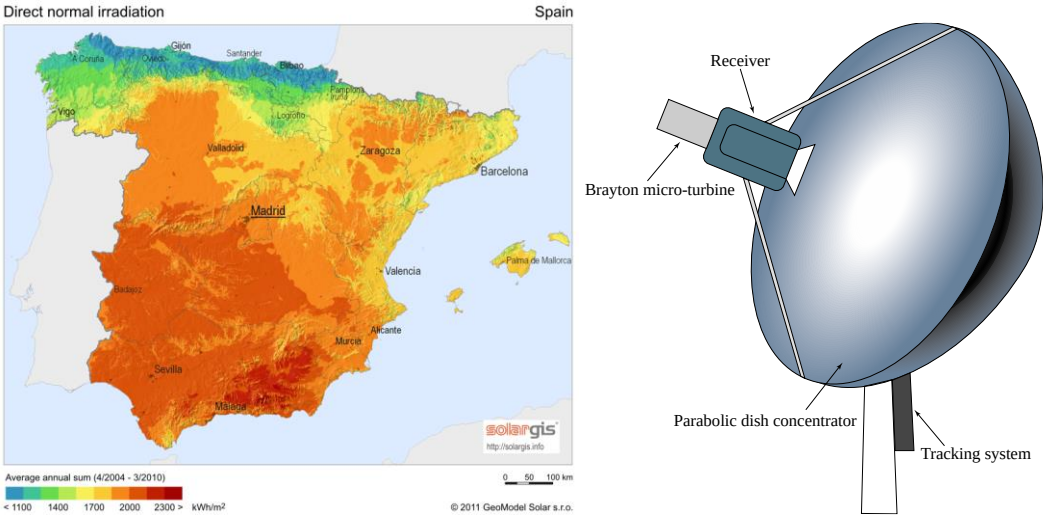

Fig. 1. Direct normal irradiance, G, map for Spain [5] (left) and outline of the different components of the parabolic dish (right).

- The *concentrator* or optical device is the parabolic mirror that redirects the radiation to the receiver. Depending on the thickness and the materials used, the solar mirrors have reflection performances between 90 and 94%. This fact, together with the high concentration ratios of parabolic dishes (typically 600 – 2.000), makes them one of the most efficient systems for obtaining electric energy from the Sun [4,6].
- The *receiver* is the element of the system where the radiation is absorbed and transferred to the fluid performing the thermodynamic cycle [6].
- The *micro gas-turbine*, located in the focal point of the parabolic dish, is a small hybrid recuperated gas-turbine comprising one compressor, an auxiliary combustor, one expander, a recuperator and a high speed alternator [7].
- The *solar tracking mechanism* is the system that allows to arrange the concentrator approximately in a normal way to the direction of propagation of solar radiation. It involves a mechanical system and a control system to make a movement in two axes.

1.2. Distributed energy

Distributed generation refers to a variety of technologies intending to generate electricity at or near where it will be used. Distributed generation may serve a single structure (such as a home or business), or it may be part of a micro grid (a smaller grid that is also tied into the larger electricity delivery system). When connected to the electric utility's lower voltage distribution lines, distributed generation can contribute to support delivery of clean, reliable power to additional customers and to reduce electricity losses along transmission and distribution lines [8].

The modularity and size of the hybrid parabolic dish system coupled with a micro-gas turbine allows it to operate individually for remote applications or to be connected to the electric network, with the advantage of producing a stable output power for 24 hours a day, 365 days of the year.

1.3. Objectives

The first objective of this work is to present a general thermodynamic model for a hybrid system consisting of a parabolic dish and of a Brayton micro gas turbine. The model has been worked out with *Mathematica*® and it is based on previous works for solar concentration towers developed by our group [9,10]. One of the key points of the model is its capability to perform off-design analysis. The dynamical evolution of any plant output parameter (efficiencies, temperatures, solar share, power output, instantaneous fuel consumption, etc.) can be obtained, for any real curve of irradiance and ambient temperature. Moreover, an analysis on the importance over overall plant records of particular variables of each subsystem can be readily developed.

Because of the difficulty of finding a complete set of real systems data and in order to check the validity of the model, results from this study are compared with those obtained by Semprini *et al.* [3] for four output power levels (30, 23, 15 and 7 kWe) operating only with solar input.

Afterwards, an analysis of hybrid and sunless performance is carried out for four different micro gas-turbine power outlets and for four days of the year (corresponding to the four seasons). Another important objective is to simulate and to predict the behaviour of the plant over time, calculating the daily curves of the output parameters. An analysis on a particular illustrative day will be shown. In addition, fuel consumption and emission of pollutant gases into the atmosphere associated with the production of electric energy are estimated.

2. Thermodynamic model

2.1. Scheme of the plant

Figure 2 shows the scheme of the considered hybrid thermo-solar power plant. It consists of three main subsystems: the solar collector, the combustion chamber and the power block assumed to be a recuperative Brayton gas turbine.

In the solar collector (orange colour in Fig. 2), an energy flow GA_a is received, where G is the direct normal solar irradiance or energy received per unit of time and surface and A_a is the aperture area of the parabolic dish (cross sectional area of the aperture plane). The reflection towards the solar receiver is not perfect, there are losses defined by the optical efficiency, η_0, and due to factors such as air absorption, humidity, dirt in the mirrors or shadow effects. The solar receiver collects this energy and transfers it (as a heat exchanger) to the working fluid developing the thermodynamic cycle. Heat losses in the receiver are accounted.

From the combustion chamber (red colour in Fig. 2), an energy flow $\dot{m}_f \cdot Q_{LHV}$ could be released. It is determined by the fuel flow, $\dot{m}_f$, and by the lower heating value per unit mass, Q_{LHV} (energy per unit of mass contributed by the fuel). The necessary fuel flow varies depending on the solar time, the time of year, and the weather conditions since it must rectify the oscillations of the irradiance. In the chamber, at mean temperature, T_{HC}, there are losses caused by the incomplete combustion of natural gas and by heat dissipation in the walls. The chamber transfers heat flow to the working fluid through another non-ideal heat exchanger because the combustion is considered as external. In

other words, the Brayton thermodynamic cycle developed by the working fluid is closed, avoiding turbine blades degradation.

In the thermal power block (black colour in Fig. 2), pressurized air with an average heat capacity, c_w, and an adiabatic coefficient, γ, independent of temperature (actually the model allows for the consideration of temperature dependent heat capacities [10], but considering average values does not change appreciably the results), performs the Brayton thermodynamic cycle, which consists of four stages:

1. First, the gas is compressed increasing its pressure and temperature from T_1 to T_2.

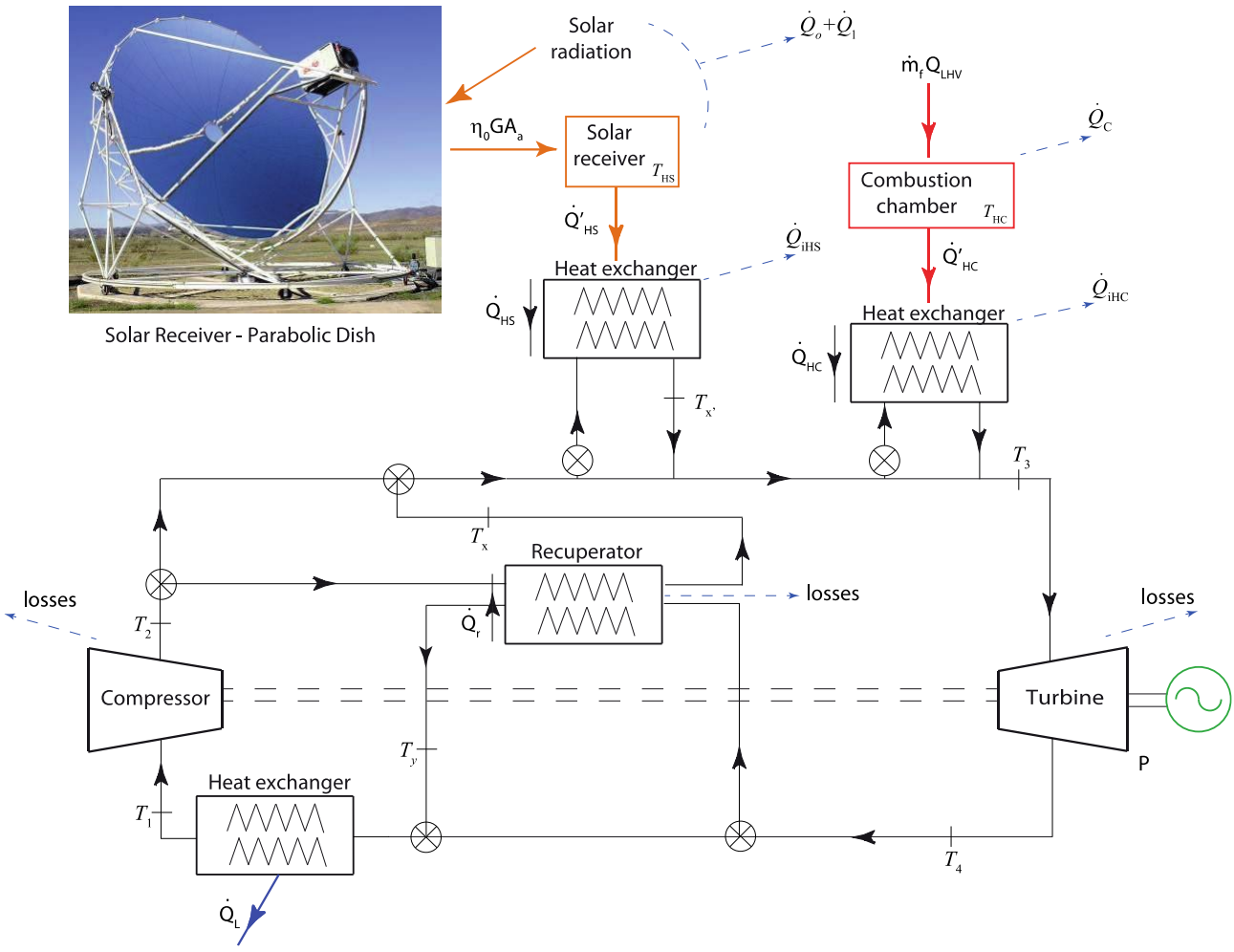

Solar Receiver - Parabolic Dish

Fig. 2. Scheme of the hybrid solar micro gas-turbine plant considered.

2. Subsequently the air temperature is increased by several heat inputs: first with heat input coming from a recuperator, which is a heat exchanger device used to take advantage of the residual heat after expansion. It raises the temperature up to T_x. Second, the heat flow coming from the solar receiver increases the mass flow temperature up to $T_{x'}$. And third, the one transferred by the combustion chamber (if necessary) increases the air up to the inlet turbine temperature, T_3. This temperature is considered approximately constant, so that the power output of the plant will also be approximately constant.
3. Then, the gases expand in the turbine, generating mechanical energy, which is transformed into electrical energy by an electric generator. At the exit of the turbine, the air temperature has decreased up to T_4.
4. To close the cycle, the air should return to its initial temperature T_1, so the excess heat is to be released. First, the recuperator at the exit of the turbine takes advantage of some of this extra thermal energy to increase the temperature of the gas at the compressor exit. After the

recuperator, the temperature is T_y. To reach T_1, additional heat is transferred to the ambient through another heat exchanger.

Along the overall process the main irreversibilities are taken into account, both external losses (associated with the coupling of the thermal device with the surroundings through the heat exchangers) and internal losses (associated with inherent irreversibilities as pressures drops and non-ideal isentropic efficiencies in the compressor and turbine).

Heat input and heat release in the plant are schematized in Fig. 2. The solar collector gets a solar power GA_a, $\dot{Q}_0$ represents the optical losses at the solar subsystem, and $\dot{Q}_l$ losses associated to the receiver, including radiation and convection/conduction heat transfer terms [11]. The heat exchanger associated with the receiver gets $\dot{Q}'_{HS}$ and has some losses, $\dot{Q}_{iHS}$, so it transfers to the working fluid an effective heat flow $\dot{Q}_{HS}$. The effectiveness of the receiver considered as a heat exchanger, ε_{HS}, is defined as the ratio between the energy flow actually transferred and the one that would be transferred if it worked ideally.

The combustion chamber receives a maximum energy flow $\dot{m}_f \cdot Q_{LHV}$ and transfers $\dot{Q}'_{HC}$ to its heat exchanger. This heat exchanger also has some losses that are given by $\dot{Q}_{iHC}$. Its effectiveness is denoted as ε_{HC}. The thermal engine receives a heat flow input from the combustion chamber $\dot{Q}_{HC}$. Therefore, the total heat received from the two external sources is the sum $\dot{Q}_{HS} + \dot{Q}_{HC}$.

2.2. Global thermal efficiency of the plant

The thermal engine releases to the environment a heat $\dot{Q}_L$ and produces a power P, given by the difference between the absorbed heats $(\dot{Q}_{HS} + \dot{Q}_{HC})$ and the one that yields $\dot{Q}_L$. A detailed model can be consulted in [9,10]. Here only some relevant energetic parameters are summarized.

The solar share, *f*, is the fraction of the energy absorbed by the working fluid that comes from the solar subsystem, as it is expressed in (1),

$$f = \frac{|\dot{Q}_{HS}|}{|\dot{Q}_{HS}|+|\dot{Q}_{HC}|}. \quad (1)$$

The overall thermal efficiency is defined in (2) as the ratio between the delivered net power and the total heat input,

$$\eta = \frac{P}{G\,A_a + \dot{m}_f\,Q_{LHV}}. \quad (2)$$

This efficiency can also be expressed as a combination of the efficiencies of the plant subsystems (solar η_s, combustion η_c, and gas turbine η_h), the effectivenesses of the heat exchangers connecting subsystems (ε_{HS} for solar subsystem and ε_{HC} for combustion subsystem) and the solar share, *f*. Thereby the overall efficiency of the whole system, η, is given by (3) (see [9,10] for details):

$$\eta = \eta_h \eta_s \eta_c \left[\frac{\varepsilon_{HS}\,\varepsilon_{HC}}{\eta_c\, f\, \varepsilon_{HC} + \eta_s\,(1-f)\,\varepsilon_{HS}}\right]. \quad (3)$$

It can be also defined a fuel conversion rate or economic performance (see (4)), η_e, as the ratio between the power output and the amount of necessary heat associated with economic cost, that is, the one corresponding to the combustion chamber,

$$\eta_e = \frac{P}{\dot{m}_f\,Q_{LHV}}. \quad (4)$$

It should be noted that η_e is not a proper thermodynamic efficiency, since it is defined from 0 to infinity.

3. Numerical implementation and validation

Once the model is described, its validation is the next step. This is not easy because these systems are still in R & D & I process and there are not many available real data. For this reason, this study starts from the results recently presented by Semprini *et al.* [3] for four systems with different

output power (30, 23, 15 and 7 *kWe*), working only with solar input. These results are compared with those obtained from this model.

3.1. Numerical implementation

The main parameters that are assumed to implement in the system are summarized in Table 1. In this table the parameters are grouped by its corresponding subsystem, so ε_c is the isentropic efficiency of the compressor, D_r is the diameter of the aperture area of the receiver, η_0 is the concentrator optical efficiency, ε_t is the isentropic efficiency of the turbine, ε_r is the recuperator effectiveness, ε_L is the cold side heat exchanger effectiveness, and ρ_h and ρ_c measure the irreversibilities due to pressure drops in the heat input and in the heat release, respectively. The concentration ratio is the ratio between aperture and receiver areas, $C=A_a/A_r$. Four possible output powers are considered: 30, 23, 15 and 7 *kWe*. Pressurized air will be taken as working fluid undergoing the thermal cycle. Gas mass flow is fitted to reach those power levels, it varies from 0.0881 kg/s for a power about 7 kWe to 0.338 kg/s for the largest power output. The turbine inlet temperature was fixed at about 1170 K.

Table 1. Parameters that are taken from Semprini et al.[3] both for the validation of the theoretical model and the realization of the study for four different micro-turbine power outlets

Subsystems			*Study cases*			
			P=30 kWe	P=23 kWe	P=15 kWe	P=7 kWe
Compression	Compressor	ε_c	0.77	0.76	0.76	0.76
Solar subsystem	Collector	A_a (m^2)	211.8	169.4	109.6	52.80
		D_r (m)	0.3879	0.3480	0.2810	0.1941
		C	1792	1781	1767	1784
		η_0	0.9083	0.9087	0.9092	0.9086
	Heat exchanger	ε_{HS}	0.7951	0.7937	0.7926	0.7923
Combustion subsystem	Combustion chamber	η_c	0.97	0.97	0.97	0.97
	Heat exchanger	ε_{HC}	0.97	0.97	0.97	0.97
Expansion	Turbine	ε_t	0.76	0.76	0.75	0.74
Recuperation	Recuperator	ε_r	0.85	0.85	0.85	0.85
Cooling	Heat exchanger	ε_L	1	1	1	1
Pressure drops	Process 2→3	ρ_h	0.98	0.98	0.98	0.98
	Process 4→1	ρ_c	1	1	1	1

3.2. Validation

An estimation of the results of the solar thermal plant in static conditions can be carried out. For the *ambient temperature* the value T_L=298.15 *K* is taken and for the solar irradiance, G=780 *W/m*^{2}, which are the values that Semprini *et al.* [3] establishes. These values allow the system to work on only solar conditions. The obtained output parameters and efficiencies (expressed as relative deviations with respect to the results from [3]) are shown in Table 2. It can be seen that the overall returns of the system fairly fit the results by Semprini *et al*. [3], deviating between 6.7% and 7.8%. Thermal efficiencies of the Brayton heat engine, η_h, are approximately constant for all four cases. The power levels generated by the turbine, *P*, are the results showing the greatest differences with respect to the reference values. Note also in Table 2 that the case P = 30 kW is the one with best fit in all outputs. The differences found between this model and that in [3] are acceptable (less than 10%) taking into account that this is a first approximation (average heat capacities were assumed),

and that the study of Semprini is quite more detailed in which refers to heat exchangers and solar receiver.

Table 2. Relative deviations for the four different micro turbine power outlets (30, 23, 15, and 7 kWe), for fixed solar irradiance and ambient temperature when comparing with the results by Semprini et al [3].

Power outlet, P (kWe)	30	23	15	7
T_L (K)	298.15	298.15	298.15	298.15
G (W/m^2)	780	780	780	780
Relative deviations				
$\Delta\eta$ (%)	6.74	7.73	7.77	7.79
$\Delta\eta_h$ (%)	8.2	8.83	8.86	8.89
ΔP (%)	7.4	9.43	9.25	9.3

4. Results

Once it was shown a satisfactory validation for particular conditions, some predictions will be presented. Starting only from two input data, irradiance, G, and ambient temperature, T_L, and the parameters detailed in Table 1, all the output records of the plant can be obtained, with the help of the equations developed in the model [9,10].

4.1. Comparative study by seasons

In this section, a study of the power plant is carried out in terms of the variation of environmental conditions throughout the year. To get this, four representative days of the year are chosen, corresponding to spring (March 21st), summer (June 20th), autumn (September 21st), and winter (December 21st) during 2013. Table 3 shows the values of G and T_L for the four days. For each one two hours are studied: at midday (12 hours, hybrid or purely solar mode) and at midnight (0 hours, only combustion mode). Assumed data are real (not smoothed nor averaged) and taken from the records carried out by the company Meteosevilla [12] from Seville, Spain. As can be seen in Fig. 1 (left) Seville is, a priori, a good location for solar plants because of its average normal direct irradiance, above 2000 kWh/m^2.

Table 3. Ambient temperature, T_L, and direct solar irradiance, G, data for the four days of the year, at midday and at midnight.

Season	*Winter*		*Spring*		*Summer*		*Autumn*	
Day	December 21st		March 21st		June 20th		September 21st	
Hour	0 h	12 h	0 h	12 h	0 h	12 h	0 h	12 h
T_L (K)	280.35	282.95	284.55	287.75	294.05	296.55	299.95	299.35
G (W/m^2)	0	418	0	741	0	760	0	586

As a summary of the study, the values of the different subsystems efficiencies (η, η_s, η_h, and η_e) are presented in Fig. 3 for the four considered power levels and for both working modes: hybrid and without sun. Each season has been assigned a colour and a symbol. The solar collector efficiency, η_s, versus P (Fig. 3(a)) has a maximum around 17 kWe, with small differences (note the scale of the vertical axis) between winter and the other three seasons (around 0.2%). Of course, the solar yield is zero at night, as there is no solar input. Figures for the solar share, f, are not shown, but for those ambient temperatures, solar irradiance and turbine inlet temperature, it never reaches f=1, *i.e*, the turbine always works with the help of the combustion chamber. To reach only solar functioning (as in paper [3]), at least irradiance values about 780 W/m^2 would be required.

The thermal efficiency of the Brayton heat engine, η_h, versus P (Fig. 3(b)) becomes greater as the generated power increases, for all seasons. In the considered interval of power outputs, the heat engine efficiency increases about 7.5 %. The overall performance, η, against P (Fig. 3(c)) behaves again like that of the turbine, η_h: increases with the power output but is greater for the pure

combustion mode than for the hybrid mode, and it does so for each season. The global increase is about 5.2 %. For pure combustion, there are no losses arising from the solar subsystem, and so overall plant efficiency is larger. It should be noted that it is in winter, when the solar irradiance and the ambient temperature have the minimum annual values, when the overall performance of the system is maximized.

The fuel conversion rate of the system, η_e, versus P (Fig. 3(d)) is significantly affected in the hybrid mode in summer and spring since a part of the heat that is introduced into the heat engine comes from a source of energy that has no economic cost. Besides, these seasons present a large increase in the performance for the highest power. Opposite, small values and small variations of η_e are observed in hybrid operation for winter and autumn (due to the scarce solar irradiance).

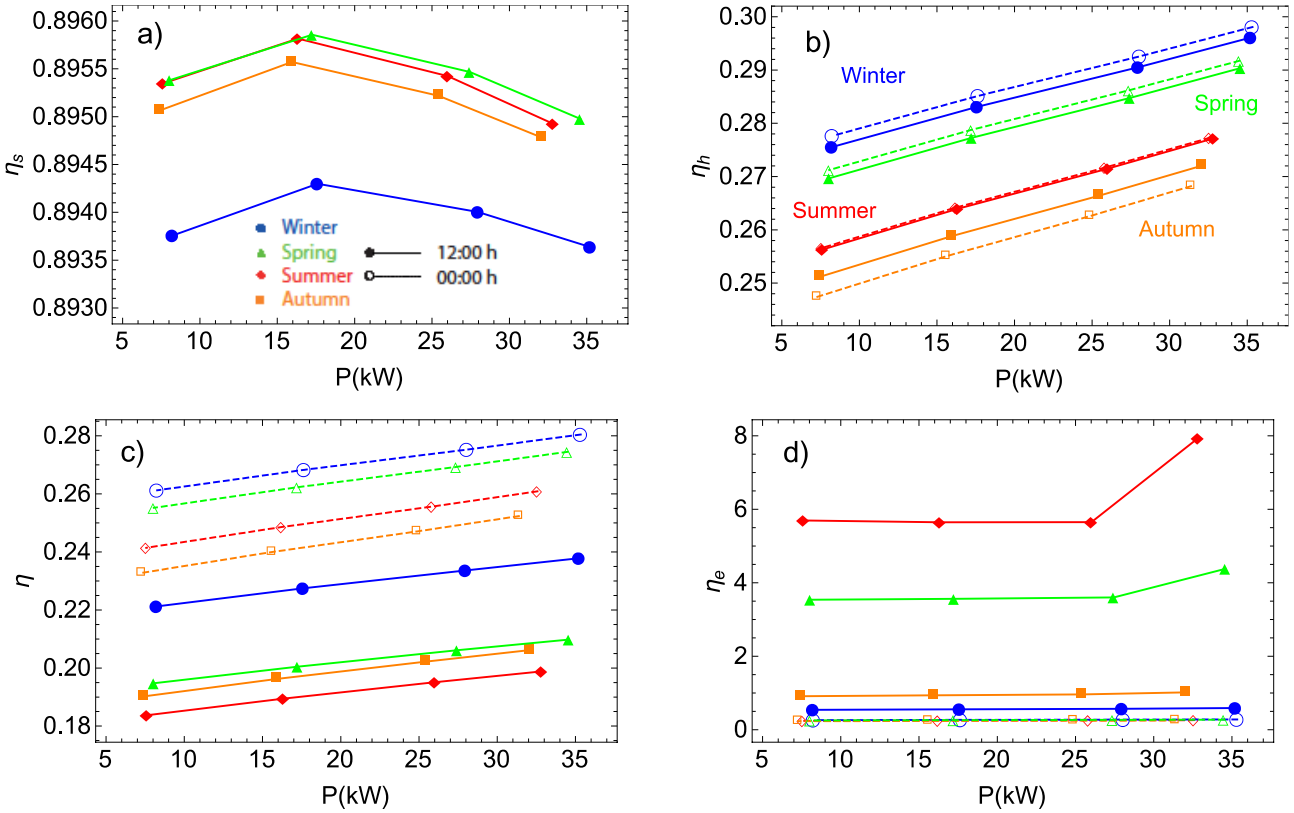

Fig. 3. Thermal efficiencies: solar collector efficiency, η_s, Brayton heat engine efficiency, η_h, overall thermal efficiency, η, and fuel conversion rate, η_e, in function of the power, for the four days of the year. Summer (red rhombuses), spring (green triangles), autumn (orange squares) and winter (blue circles). Filled symbols refer to noon (12 hours) and empty symbols refer to midnight (0 hours).

4.1.1. Fuel consumption and emissions

Figure 4(a) shows fuel consumption as a function of power, for a representative day of each season. The fuel consumption behaviour complements the one observed before for η_e: it increases with the power output in hybrid mode being more affected in winter and autumn due to the lower available irradiance. By night fuel consumption depends only on ambient temperature. The fuel saving between night and noon is around 52% in winter, 74% in autumn, 93% in spring, and 96% in summer. Thus, even under unfavourable solar conditions, fuel savings are very remarkable.

The fossil fuel plants working on Brayton cycles with natural gas are the cleanest ones since they do not emit sulphur or derivatives, although they do produce other pollutant emissions, specifically greenhouse gases. Emissions for three gases have been analyzed: carbon dioxide, CO_2; methane CH_4; and nitrous oxide, N_2O, because they are the main greenhouse gases associated with the combustion of natural gas.

Figure 4 (b) shows, as an example, the results of CO_2 emissions, for the 4 power output levels considered, for December 21st. The situation is compared at 12 and at 00 h. It is observed that the

reduction of pollutant emissions is about 50% in hybrid mode, for this day, which would be the most unfavourable since the solar contribution is lower than in any other season. To calculate the results, standard emission factors for natural gas have been used [13].

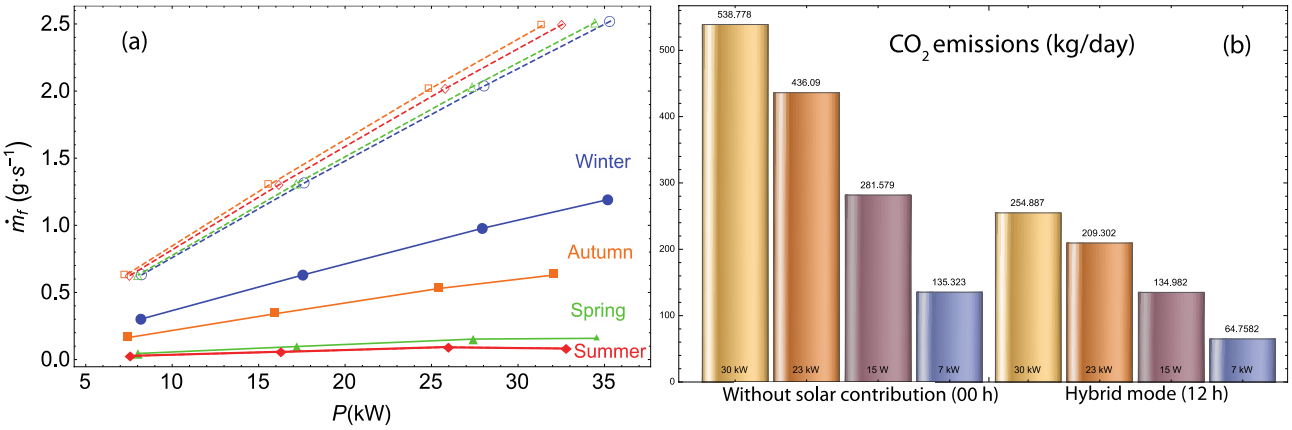

Fig. 4. (a): Fuel consumption as a function of power, for a representative day of each season. Hybrid mode, at 12 h (filled symbols) and running without sun, at 00 h (empty symbols). (b): Graphical representation of the CO_2 emissions on December 21st at midnight (00 h) and at midday (12 h) for the four power cases.

4.2. Dynamic study

In order to get dynamic information of the power plant, irradiance and ambient temperature data are selected from Seville, Spain, every 30 minutes, for December 21st 2013, provided from a database of the company Meteosevilla [12]. The choice of a winter day is made in order to highlight the advantages of this type of plants by considering a day of the year, in principle, with few sunlight hours and small irradiance peak values. Input data are real, not averaged nor smoothed to stress the noise due to fluctuating weather. The most relevant results are presented below.

4.2.1. Irradiance and ambient temperature

Figure 5(a) shows the irradiance, G, and the ambient temperature, T_L, versus time, t, for a representative winter day. When observing this figure, it is clear that the irradiance is null at night and begins to grow at dawn, reaching its maximum value in the central hours of the day. Then, it decreases and is cancelled again at nightfall.

Two fundamental factors stand out in the behaviour of irradiance:

- On the one hand, the width of the curve or number of hours of sun, about 10 hours for this winter day (the maximum would be about 15 hours in summer).
- And, on the other hand, the height of the curve or maximum irradiance, which is received in the central hours, and ranges, for instance in Seville, from 470 W/m^2 in winter to 910 W/m^2 in summer. It should be remembered that Semprini *et al.* [3] considers 780 W/m^2 (Table 2) as the optimum value for the operation of the micro gas turbine without the contribution of fossil fuel.

The shape of the graph of the ambient temperature is sinusoidal, in the first hours of the day it decreases taking the minimum at dawn and growing up thererafter. In Seville the lowest temperatures of the year are reached in winter. The ambient temperature is out of phase with respect to irradiance.

4.2.2. Power output

Figure 5(b) shows the evolution versus time of the overall thermal efficiency, η, and the power output, P, for the selected day. In this figure it can be seen that the power output is not strictly constant, but it oscillates with maximum amplitude variations of about 2 kW. This means that one of the premises in the design of this kind of installations is fulfilled: to rectify the oscillations of the irradiance after the collector in order to obtain a practically constant power output. The existing

small amplitude oscillations are due to those of the ambient temperature, which have not been corrected. These oscillations are in counterphase with respect to T_L. However, the oscillations of the overall thermal efficiency, η, are due both to those of the irradiance and to those of the ambient temperature.

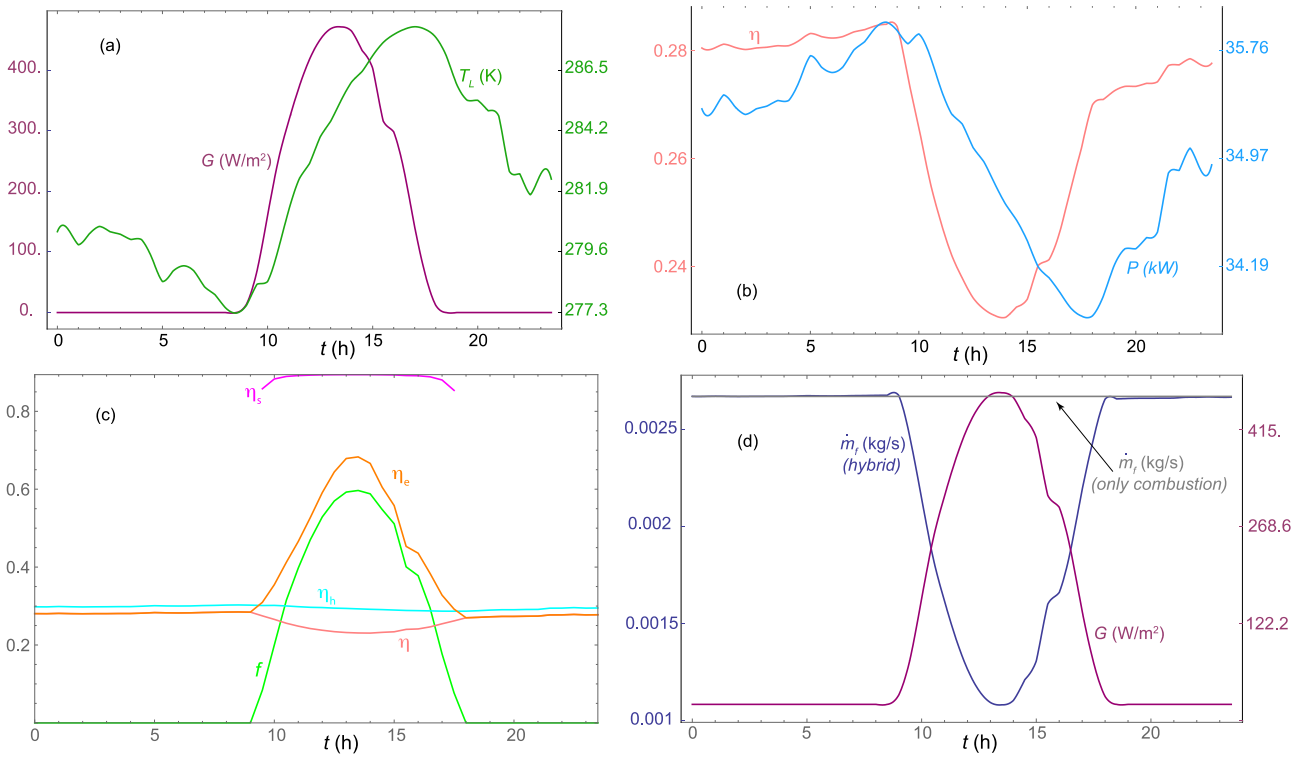

Fig. 5. (a) Direct normal irradiance, G, and ambient temperature, T_L, for December 21st 2013; (b) calculated overall efficiency, η, and power output, P; (c) different efficiency values and solar share, f; and, (d) fuel consumption and solar irradiance. Time is represented in UTC hours.

4.2.3. Efficiencies and solar share

In Fig. 5(c), the overall plant efficiency, η, the solar collector efficiency, η_s, the thermal efficiency of the Brayton heat engine, η_h, the fuel conversion rate, η_e, and the solar share, f, are plotted against time, for the considered winter day. As shown in this figure, solar collector efficiency, η_s, is not defined at night and its behaviour during the hours of insolation is dominated by the optical efficiency of the collector. For this reason it is practically constant with a value around 0.89, always lower than 0.91 (the value of η_0) and modulated by the heat losses in the collector. The width of the plateau is a straight consequence of the number of insolation hours.

The thermal efficiency of the Brayton heat engine, η_h, takes values around 0.29 and varies very smoothly because the turbine inlet temperature, and so the total heat input, is almost fixed, independently of the way heat is produced, solar radiation or combustion. Existing very flat variations are only associated with external temperature fluctuations. The overall plant efficiency, η, remains constant at night, when η_s is not defined, and decreases during the hours of insolation because of the irreversibilities of the combined system (see (3)).

At night, the fuel conversion rate, η_e, corresponds to the global one because there is no solar contribution and when there is sufficient irradiance it varies opposite to G. This is obviously associated with the fact that in the central hours the solar share reaches maximum values and thus, the fuel consumption is minimal.

4.2.4. Fuel consumption and emissions

Fuel consumption is constant at night, when it takes its highest value because there is no solar contribution. During the daytime, it varies inversely with solar irradiance. This can be seen in Fig. 5(d), which represents the flow of fuel consumption with solar input, $\dot{m}_f$, without solar contribution

(grey line) and irradiance, *G*, versus time, *t*. As expected, at dawn, consumption begins to drop until it reaches its minimum value when the irradiance is maximum, in the central hours of the day. This drop in consumption represents 14% in winter. The fuel flow without solar contribution is approximately constant and numerically around 0.0026 kg/s, while with solar contribution it is maximum in winter due to the low irradiance. This saving in fuel logically translates into a decrease in pollutant emissions.

5. Conclusions

The most important conclusions from this work are summarized below:

- A non-stationary (off-design) thermodynamic model has been developed, with analytical equations, for a power generation plant based on the hybridization of a parabolic dish solar collector and a Brayton gas turbine micro-cycle operating in a closed cycle. Losses or irreversibilities in each of the subsystems and in the heat exchangers are considered.
- The system is described from the thermodynamic point of view with a reduced number of parameters, each one of clear physical significance.
- The model has been validated using the previous work by Semprini *et al.* [3].
- A study was carried out for real values of fixed direct normal irradiance, *G*, and ambient temperature, T_L, considering four representative days of the year, corresponding to all seasons and two hours of the day: at midnight and at midday and four different power outputs, *P*: 30, 23, 15, and 7kWe.
- A dynamic study has also been carried out, with real *G* and T_L values, as a function of time, throughout a particular day taken as an illustration. This model allows to track any parameter of the system as a function of time.
- The number of hours of insolation has been decisive in the daily evolution of plant efficiency curves.
- The fuel conversion rate presents a parabolic behaviour and shows a maximum in the hours of maximum insolation or central hours of the day.
- The power output of the plant remains approximately constant for any solar and meteorological contribution conditions; therefore, the objective that the supply of electric power does not depend on meteorological conditions has been fulfilled.
- This type of solar thermal power plants seems to be competitive from the point of view of saving the consumption of fossil fuels and pollutant emissions in regions with high solar radiation and low availability of water.
- The realization of thermoeconomic works is needed for further development of the parabolic dish power plants and its commercial implementation in order to properly accomplish their objective: the production of efficient and clean electric energy in a distributed way.

Acknowledgment

The authors acknowledge financial support from JCYL of Spain, Grant SA017P17

Nomenclature

A_a	aperture area of the solar field, m^2	$\dot{m}_f$	fuel mass flow rate, kg/s
C	solar collector concentration ratio	P	power output, MW
c_w	average heat capacity, $J/(kg\ K)$	Q_{LHV}	fuel lower heating value, MJ/kg
f	solar share	t	time, h
D_r	receiver aperture area diameter, m	T_{HC}	combustion chamber temperature, K
G	direct solar irradiance, W/m^2	T_L	ambient temperature, K

Greek symbols

γ adiabatic coefficient

η overall thermal efficiency

η_c combustion chamber efficiency

η_e fuel conversion rate

η_h heat engine thermal efficiency

η_s solar collector efficiency

η_0 concentrator optical efficiency

ε_c compressor isentropic efficiency

ε_r recuperator effectiveness

ε_t turbine isentropic efficiency

ε_L cold side heat exchanger effectiveness

ε_{HC} combustion chamber heat exchanger effectiveness

ε_{HS} collector heat exchanger effectiveness

ρ_c irreversibilities due to pressure drops in the heat release

ρ_h irreversibilities due to pressure drops in the heat input

References

[1] https://www.unfccc.int/paris_agreement/items/9485.php [accessed 31.1.2018]

[2] Asociación Española de la Energía Termosolar. Available at: <http://www.protermosolar.com> [accessed 21.1.2018]

[3] Semprini S., Sánchez D. and De Pascale A., Performance analysis of a micro gas turbine and solar dish integrated system under different solar-only hybrid operating conditions. Sol. Energy 2016; 132:279-293.

[4] Aichmayer, L., Spelling, J., and Laumert, B. Preliminary design and analysis of a novel solar receiver for a micro gas-turbine based solar dish system. Sol. Energy 2015; 114, 378-396.

[5] GeoModel Solar. Direct Normal Irradiation map. Solargis Available at: < www.solargis.com> [accessed 26.1.2018]

[6] Giostri, A. and Macchi, E. An advanced solution to boost sun-to-electricity efficiency of parabolic dish. Sol. Energy 2016, 139:337-354.

[7] Gavagnin, G., Sánchez, D., Martínez, G.S., Rodríguez, J.M., and Muñoz, A. Cost analysis of solar thermal power generators based on parabolic dish and micro gas turbine: Manufacturing, transportation, and installation. Appl. Ener. 2017, 194:108-122.

[8] EPA United States Environmental Protection Agency. Available at: <https://www.epa.gov/energy/distributed-generation-electricity-and-its-environmental-impacts> [accessed 21.1.2018]

[9] Olivenza-León D., Medina A., and Calvo Hernández A., Thermodynamic modelling of a hybrid solar gas-turbine power plant. Energ. Conv. Manage 2015; 93: 435-447.

[10] Santos M.J., Merchán R.P., Medina A., and Calvo Hernández A., Seasonal thermodynamic prediction of the performance of a hybrid solar gas-turbine power plant. Energ. Convers. Manage 2016; 115: 89-102.

[11] Duffie J.A., Beckman, W.A., Solar Engineering of Thermal Processes. Hoboken, NJ, USA: John Wiley and Sons; 2006.

[12] Meteosevilla. Available at:<http://www.meteosevilla.com> [accessed 21.1.2018]

[13] Emission factors for greenhouse gas inventories. Available at:<https://www.epa.gov/sites/production/files/2015-07/documents/emission-factors_2014.pdf> [accessed 21.1.2018]